DOI:10.1190/segam2019-3215437.1

A brief analysis of MobileMT data

Daniel Sattel, EM Solutions, Ken Witherly, Condor Consulting and Vlad Kaminski, Aarhus Geophysics*

Summary

The MobileMT system measures natural-field EM data, acquiring three-component airborne magnetic-field data while monitoring the horizontal electric field at a base station. Data sensitivities of this configuration are similar to those of TE-mode MT data. Synthetic 2D modeling results across a conductive body demonstrate how the host conductivity and the location of the base station affect the conductor response. The strong sensitivity of the data to the conductivity structure at the base station results in inversion results being quite sensitive to the inversion start models used.

MobileMT survey data from the Grindstone Copper-Nickel-Cobalt project, New Brunswick indicate a strong correlation between conductivity highs and magnetic anomalies. 2D inversions suggest conductivity structures to be detected up to 1000-2000 m depth. Model results from a VMS exploration survey across the Broken Evil prospect, Northern Ontario show good correlation with conductivity structures derived from a previous VTEM survey, including the location of a suspected VMS body.

Introduction

Natural-field EM data can be acquired and processed in various ways. The magnetotelluric (MT) method measures electric and magnetic-field data on the ground, followed by the derivation of impedance tensors or apparent resistivity and phase data. Alternatively, tipper vector data can be derived from the magnetic-field data, if vertical-component data were acquired. Various airborne adaptations of the MT method have been developed, including airborne AFMAG (Ward, 1959), the ZTEM and AirMt systems, operated by Geotech (Legault, 2012) and the recently developed MobileMT system, shown in Figure 1, operated by Expert Geophysics. Some parameters of these systems are summarized in Table 1.

The ZTEM system takes airborne measurements of the vertical magnetic-field data, while horizontal magnetic-field data are recorded at a base station. The AirMt system measures three-component magnetic-field data with an airborne sensor and at a base station. The MobileMT system acquires airborne three-component magnetic-field data while recording the horizontal electric-field data at a base station. As a result of the different system configurations, data sensitivities to subsurface conductivity structures differ significantly between these systems.

After a brief description of the MobileMT system, synthetic data models are discussed in order to demonstrate the sensitivities of MobileMT data to a range of conductivity scenarios. Then, modeling results from survey data acquired 2018 across the Grindstone Copper-Nickel-Cobalt project, New Brunswick and the VMS-gold Broken Evil prospect, Northern Ontario are discussed.

Figure 1: MobileMT system airborne sensors, including cesium magnetometer and three-component dB/dt sensor in hardshell.

	ZTEM	AirMt	MobileMT
Airborne data	dBz/dt	3C dB/dt	3C dB/dt
Recorded at base	dBx/dt dBy/dt	3C dB/dt	Ex, Ey
Airborne coil size (diameter)	7.4 m	3 m	1.4 m
Digitization frequency	2 kHz	2 kHz	98 kHz
Processed data	Tipper vector 22 – 720 Hz	Amplitude Parameter 45 – 720 Hz	Apparent conductivity 30 – 20 kHz

Table 1: Parameters of airborne NFEM systems.

10.1190/segam2019-3215437.1

MobileMT

The airborne magnetic-field data are acquired with dB/dt coils, towed by a helicopter while the horizontal electric field components are recorded by two pairs of orthogonal sensors (signal and reference) at a base station. Sampling the EM data at 98 kHz allows for the derivation of responses in the frequency range 30 Hz – 20 kHz.

The recorded magnetic and electric-field data are related to each other through the admittance tensor *Y*:

$$\begin{pmatrix} Hx \\ Hy \end{pmatrix} = \begin{pmatrix} Yxx\,Yxy \\ Yyx\,Yyy \end{pmatrix} \begin{pmatrix} Ex \\ Ey \end{pmatrix} \quad (1)$$

Next, apparent conductivity σ^{app} and phase φ can be derived from the determinant Y_{DET}:

$$Y_{DET} = \sqrt{YxxYyy - YyxYxy} \quad (2)$$

$$\sigma^{app} = \mu\omega \left| Y_{DET}^2 \right| \quad (3)$$

$$\varphi = \arg\left(Y_{DET}^2\right) \quad (4)$$

Currently only the apparent conductivity data are provided for MobileMT data sets. Further, the recorded vertical component dB/dt data might be used in the future for deriving roving tipper data.

Grids and profiles of apparent conductivity data can be directly interpreted. However, these data can be affected by topography. In order to derive conductivity-depth information, while taking into account the terrain's topography and varying sensor elevation, 2D and 3D inversions can be applied.

Synthetic modeling

For 2D modelling, the computation of the predicted Y_{DET}, σ^{app} and φ simplify to the following:

$$Y_{DET} = \sqrt{-YyxYxy} = \sqrt{-Y_{TM}Y_{TE}} \quad (5)$$

$$\sigma^{app} = \frac{1}{\sqrt{\rho_{TE}^{app}\rho_{TM}^{app}}} \quad (6)$$

$$\varphi = \frac{1}{2}(\varphi_{TE} + \varphi_{TM}) \quad (7)$$

with the subscripts *TM* and *TE* referring to the TM- and TE-mode parameters. σ^{app} and φ are independent of the strike direction and 3D and galvanic distortion effects (static shift) can be suppressed to some extent (Pedersen and Engels, 2005; Mansoori et al., 2016).

An Occam MT/ZTEM 2D inversion algorithm (Sattel and Witherly, 2012; Wannamaker et al., 1987; deGroot-Hedlin and Constable, 1990) was modified to allow for the modelling of σ^{app} and φ. The E-field base station is modelled to be located at the start of the section. Profiles of σ^{app} and φ across a 100 mS/m conductor at surface in a 1 mS/m half-space are shown in Figure 2. Since the E-field data are modelled at a fixed location, the ρ_{TM} and φ_{TM} terms are uniform along the profile and the diagnostic conductor information comes from the ρ_{TE} and φ_{TE} terms. It should be noted that for MT and VLF-R surveys, ρ_{TE} data provide poorer spatial resolution than ρ_{TM} data (Beamish, 2000); hence, as expected, the range of σ^{app} values in Figure 2 is quite small: 1 mS/m < σ^{app} < 2.2 mS/m. For comparison, σ^{app} derived for a H-field base station and a roving ground E-field receiver has a much wider range for that conductivity model: 1 mS/m < σ^{app} < 100 mS/m. The latter configuration would be much preferable, but cannot be implemented for airborne operation. The narrow response range predicted for MobileMT data suggests that the system requires high S/N levels to be feasible.

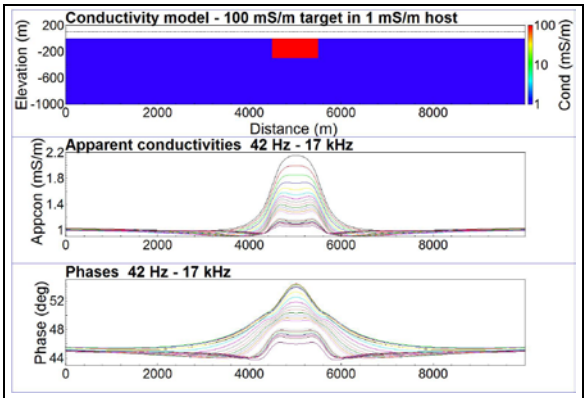

Figure 2: MobileMT apparent conductivity and phase profiles across a 100 mS/m conductor in a 1 mS/m half-space host. The H-field sensor was modeled at 100 m above the surface. Responses are shown for the frequency range 42 Hz – 17 kHz, but exclude responses in the AMT dead band (1 – 2.5 kHz).

Figure 3 shows profiles of σ^{app} across the 100 mS/m conductor of Figure 2 in a layered-earth host. The layered-earth host results in a background response that diminishes the conductor response. As shown in Figure 4, the response profile is also strongly affected, if the layered-earth cover is reduced to a patch at the base station location. In that case, the phases (not shown here) are negative and the σ^{app} conductor response at higher frequencies are similar to the background response.

10.1190/segam2019-3215437.1

DOI:10.1190/segam2019-3215437.1

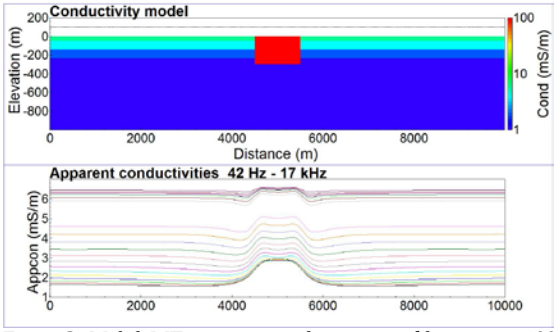

Figure 3: MobileMT apparent conductivity profile across a 100 mS/m conductor in a layered-earth host.

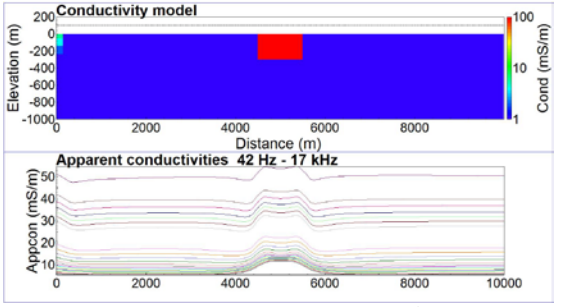

Figure 4: MobileMT apparent conductivity profile across a 100 mS/m conductor in a 1 mS/m half-space host. The base station is located on the pocket of 6 mS/m at zero distance.

Due to the strong sensitivity of σ^{app} to the conductivity structure at the base station, the success of a MobileMT data inversion depends strongly on the start model used. The inversion of the σ^{app} conductor response of Figure 2 is shown in Figure 5 for using a 1 mS/m half-space as a start model. Even though this start model agrees with the actual conductivity model at the base station location, the recovered conductivity section, while good, is not excellent. Nevertheless, the result indicates that even though the target response is much smaller than a corresponding MT response, the response exceeds the estimated noise level and the inversion recovers the conductor location.

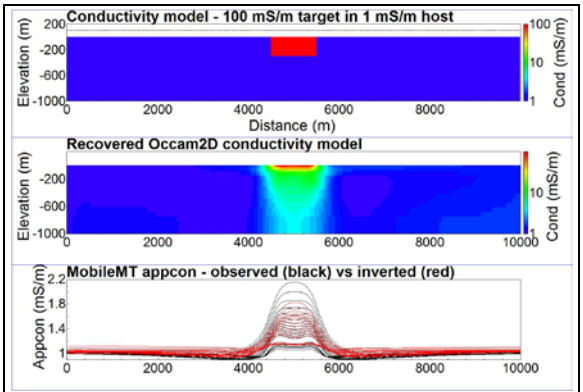

Figure 5: Inversion result of data from Figure 2, using a 1 mS/m half-space as a start model.

MobileMT survey New Brunswick

Canadian Energy Material Corp. commissioned a MobileMT survey on their Grindstone Copper-Nickel-Cobalt project, New Brunswick in 2018. The previous and current exploration efforts are described by Geominex (2018). The target area is an extended magnetic anomaly that coincides with silt geochemical Cu-Ni-Co anomalies. The exploration targets include magmatic Cu-Ni +/- PGE deposits and sediment-hosted stratabound copper deposits. Previous drill holes in the project area that targeted magnetic anomalies and VLF conductors intersected 1-2% pyrrhotite and pyrite.

The survey flightpath and the location of the base station are shown in Figure 6. The terrain clearance of the receiver coils ranged from 27 to 126 m. Apparent conductivities were provided in the frequency range 53 – 8,580 Hz, outside of the AMT dead band. Figure 6 also shows grids of the DTM, total magnetic intensity and the apparent conductivities at 4290, 268 and 53 Hz. The analysis performed by Geominex (2018) indicates a strong correlation between conductivity highs and magnetic anomalies.

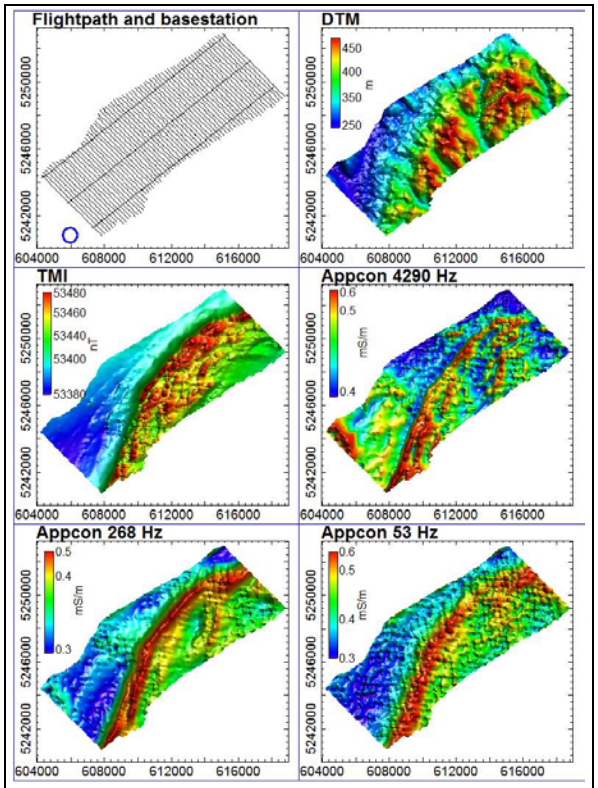

Figure 6: Survey flightpath and location of basestation, DTM, TMI and apparent conductivities at 4290, 268 and 53 Hz.

10.1190/segam2019-3215437.1

DOI:10.1190/segam2019-3215437.1

A 2D inversion result of one line of apparent conductivity data is shown in Figure 7. The top panel shows the derived conductivity-depth section. The maximum depth penetration, estimated to be 1.5 times the skin depth at the lowest frequency (Spies, 1989) is indicated on the conductivity section as a dashed line. The lower panel shows the observed and modeled apparent conductivities, indicating an excellent data fit by the inversion. Even though the observed apparent conductivity values are confined to a range of 0.3 – 0.6 mS/m, the derived conductivity section appears to suggest that structures as deep as 2000 m were detected by the data.

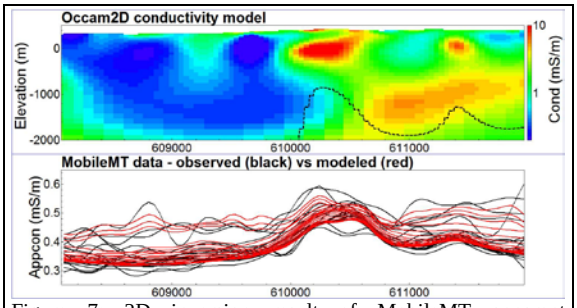

Figure 7: 2D inversion result of MobileMT apparent conductivities acquired at the Grindstone project. The black line on the conductivity-depth section indicates the estimated depth penetration of the data.

MobileMT survey Northern Ontario

MobileMT data were acquired across the Broken Evil VMS gold prospect in the Abitibi Greenstone Belt, northern Ontario in 2018. The survey area overlaps with the area of two VTEM surveys flown for Promiseland Exploration in 2007 and 2013 (Kaminski et al., 2016). A MobileMT 432 Hz apparent conductivity grid is shown in Figure 8 together with a conductivity slice at 150 m depth derived by spatially-constrained layered-earth inversion (Viezzoli et al., 2008) from VTEM data. There is excellent agreement between the mapped conductivity structures.

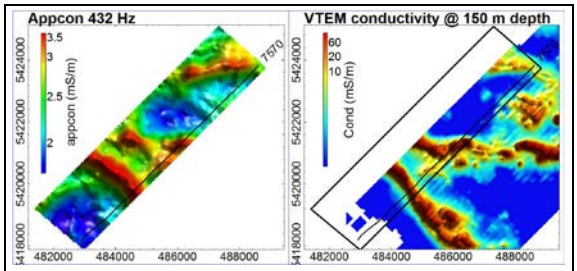

Figure 8: MobileMT apparent conductivity grid derived at 432 Hz and conductivity slice at 150 m depth, derived from VTEM data.

Conductivity-sections for line 7570, indicated in Figure 8, are shown in Figure 9. The sections were derived by 2D inversion from MobileMT data and by 1D inversion from VTEM data. Overall there is good agreement between the conductivity sections. The VTEM inversion results display some 1D artefacts, including the 'pant legs' at the edges of the anomaly at the profile center. Recent drilling within 100 m of that anomaly indicated a 15 m thick overburden and intersected a semi-massive sulfide mineralization zone at 82-103 m depth. Whereas both systems indicate the latter, the resistive overburden is mapped better by the VTEM system, suggesting higher spatial resolution by the active-source EM system.

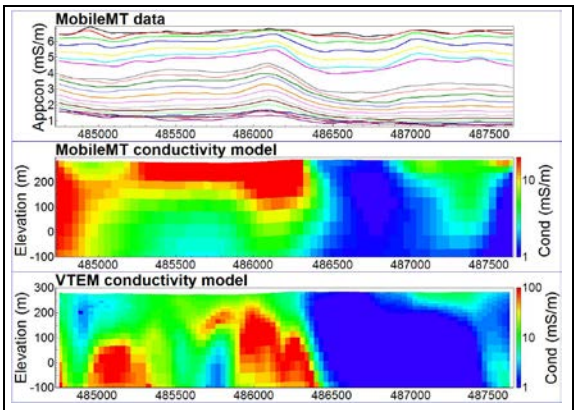

Figure 9: 2D inversion result of MobileMT apparent conductivities along line 7570. A 1D inversion of the coincident VTEM data is shown for comparion.

Conclusions

Derived from stationary E-field and airborne H-field data, MobileMT apparent conductivities are limited to a fairly narrow range of values. Nevertheless, modeling results show that detailed subsurface conductivities can be recovered successfully from synthetic and field data.

Survey data from a Copper-Nickel-Cobalt project in New Brunswick indicate a strong correlation between conductivity highs and magnetic anomalies. Survey data from a VMS gold prospect in Northern Ontario show good correlation with conductivity structures mapped by a previous VTEM survey.

Acknowledgements

We are grateful to Expert Geophysics Limited for providing feedback on the MobileMT system and to Campbell & Walker Geophysics Ltd, Canadian Energy Material Corp. and Promiseland Exploration Ltd. for providing the discussed survey data.

10.1190/segam2019-3215437.1

REFERENCES

Beamish, D., 2000, Quantitative 2D VLF data interpretation: Journal of Applied Geophysics, **45**, 33–47, doi: https://doi.org/10.1016/S0926-9851(00)00017-3.

DeGroot-Hedlin, C., and S. Constable, 1990, Occam's inversion to generate smooth two-dimensional models from magnetotelluric data: Geophysics, **55**, 1613–1624, doi: https://doi.org/10.1190/1.1442813.

Geominex, 2018, Technical Report NI43-101, Grindstone Project, Canadian Energy Materials Corp.

Kaminski, V., D. Di Massa and A. Viezzoli, 2016, Joint inversions of two VTEM surveys using quasi-3D TDEM and 3D magnetic inversion algorithms: Exploration Geophysics, **47**, 260–268, doi: https://doi.org/10.1071/EG16014.

Legault, J.M., 2012, Ten years of passive airborne AFMAG EM development for mineral exploration: 82nd Annual International Meeting, SEG, Expanded Abstracts, doi: https://doi.org/10.1190/segam2012-1267.1.

Mansoori, I., B. Oskooi, L. B. Pedersen and R. Javaheri, 2016, Three-dimensional modelling of MT data to image Sehqanat hydrocarbon reservoir in southwestern Iran: Geophysical Prospecting, **64**, 753–766, doi: https://doi.org/10.1111/1365-2478.12328.

Pedersen, L.B., and M. Engels, 2005, Routine 2D inversion of MT data using the determinant of the impedance tensor: Geophysics, **70**, no. 10, G33–G41, doi: https://doi.org/10.1190/1.1897032.

Sattel, D., and K. Witherly, 2012, An overview of ZTEM interpretation tools, *in* R. J. L. Lane, ed., Natural Fields EM Forum 2012: Abstracts from the ASEG Natural Fields EM Forum 2012: Geoscience Australia, Geoscience Australia Record.

Spies, B., 1989, Depth of investigation in electromagnetic sounding methods: Geophysics, **46**, 1137–1147.

Viezzoli, A., A. V. Christiansen, E. Auken, and K. Sørensen, 2008, Quasi-3D modeling of airborne TEM data by spatially constrained inversion: Geophysics, **73**, no. 3, F105–F113, doi: https://doi.org/10.1190/1.2895521.

Wannamaker, P.E., J. A. Stodt, and L. Rijo, 1987, A stable finite-element solution for two-dimensional magnetotelluric modeling: Geophysical Journal of the Royal Astronomical Society, **88**, 277–296, doi: https://doi.org/10.1111/j.1365-246X.1987.tb01380.x.

Ward, S. H., 1959, AFMAG–airborne and ground: Geophysics, **24**, 761–787, doi: https://doi.org/10.1190/1.1438657.